Loss Landscape Dependent Self-Adjusting Learning Rates in Decentralized Stochastic Gradient Descent

Anonymous Author(s)
Affiliation
Address
email

Abstract

Distributed Deep Learning (DDL) is essential for large-scale Deep Learning (DL) training. Synchronous Stochastic Gradient Descent (SSGD) [1] is the de facto DDL optimization method. Using a sufficiently large batch size is critical to achieving DDL runtime speedup. In a large batch setting, the learning rate must be increased to compensate for the reduced number of parameter updates. However, a large learning rate may harm convergence in SSGD and training can easily diverge. Recently, Decentralized Parallel SGD (DPSGD) has been proposed to improve distributed training speed. In this paper, we find that DPSGD not only has a runtime benefit, but also a significant convergence benefit over SSGD in the large batch setting. Based on a detailed analysis of DPSGD learning dynamics, we find that DPSGD introduces additional landscape-dependent noise that automatically adjusts the effective learning rate to improve convergence. In addition, we theoretically show that this noise smooths the loss landscape, hence allowing a larger learning rate. This result also implies that DPSGD can greatly simplify learning rate tuning for tasks that require careful learning rate warmup (e.g, Attention-Based Language Modeling). We conduct extensive studies over 18 state-of-the-art DL models/tasks and demonstrate that DPSGD often converges in cases where SSGD diverges when training is sensitive to large learning rates. Our findings are consistent across three different application domains: Computer Vision (CIFAR10 and ImageNet-1K), Automatic Speech Recognition (SWB300 and SWB2000) and Natural Language Processing (Wikitext-103); three different types of neural network models: Convolutional Neural Networks, Long Short-Term Memory Recurrent Neural Networks and Attention-based Transformer Models; and two optimizers: SGD and Adam.

1 Introduction

Deep Learning (DL) has revolutionized AI across application domains: Computer Vision (CV) [29, 14], Natural Language Processing (NLP) [50], and Automatic Speech Recognition (ASR) [15]. Stochastic Gradient Descent (SGD) is the fundamental optimization method used in DL training. Due to massive computational requirements, Distributed Deep Learning (DDL) is the preferred mechanism to train large scale Deep Learning (DL) tasks.

The degree of parallelism in a DDL system is dictated by batch size: the larger the batch size, the more parallelism and higher speedup can be expected. However, large batches require a larger learning rate and overall they may negatively affect model accuracy because (1) large batch training usually converges to sharp minima which do not generalize well [24], and (2) large learning rates may violate the conditions (i.e., the learning rate should be less than the reciprocal of the smoothness parameter) required for convergence in nonconvex optimization theory [11]. Although training longer with large batches can lead to better generalization [18], doing so gives up some or all of the speedup we seek.

[1]In the literature, SSGD is also called "Centralized Synchronized Stochastic Gradient Descent". In this paper, we use these two terms interchangeably.

Submitted to 36th Conference on Neural Information Processing Systems (NeurIPS 2022). Do not distribute.

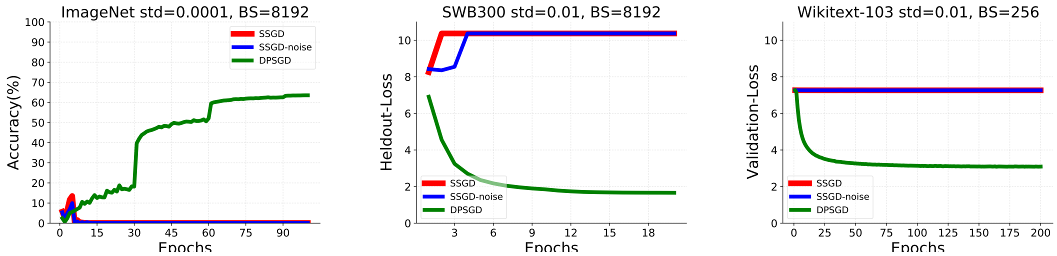

(a) VGG11-BN, ImageNet, BS8192 (b) LSTM, SWB300, BS8192 (c) GPT-2, Wikitext-103, BS256

Figure 1: SSGD (red) does not converge when the learning rate needs to be large (e.g., large batch setting or a short warmup period). Figure 1a shows model accuracy (higher is better), while Figure 1b and Figure 1c show heldout loss (lower is better). Injecting Gaussian noise (blue) does not enable SSGD to escape poor local minima. In contrast, DPSGD (green) converges using the same hyper-parameter setup. The detailed task descriptions and training recipes are given in Sections 4.3 and 4.5. BS denotes Batch-Size.

Through meticulous hyper-parameter design (e.g., learning rate schedules) tailored to each specific task, SSGD-based DDL systems have enabled large batch training and shortened training time for some challenging CV tasks [12, 54] and NLP tasks [55] from weeks to hours or less. However, it is observed that SSGD with large batch size leads to large training loss and inferior model quality for ASR tasks [58], as illustrated in Figure 1b (red curve). Here, we found for other types of tasks (e.g. CV and NLP) and DL models, large batch SSGD has the same problem (Figures 1a and 1c).

Several SSGD variants have been proposed to address large batch training problems: (1) local SGD, i.e., SGD-based algorithms with periodic averaging, where learners conduct global averaging after multiple steps of gradient-based updates [13, 36, 64]; (2) SSGD based algorithm with second-order statistics, including adaptive gradient algorithms [55, 54] and algorithms for exploring the information from the gradient covariance matrix [51]; and (3) SSGD-based algorithms on a smoothed landscape [35, 9], in which specifically designed loss landscape smoothing algorithms are used. All of these approaches require global synchronization and/or global statistics collection, which makes them vulnerable to stragglers.

Decentralized algorithms, such as Decentralized Parallel Stochastic Gradient Descent (DPSGD) [33], are surrogates for SSGD in machine learning. Unlike SSGD, where each learner updates its weights by taking a global average of all learners' weights, DPSGD updates each learner's weights by taking a partial average (i.e., across a subset of neighboring learners). In contrast to the existing variants of SSGD, DPSGD requires no additional calculation and no global synchronization. Traditionally DPSGD is a second-choice to SSGD, and is used only when the underlying computational resources are less homogeneous (i.e., a high latency network or computational devices running at different speeds). Little thought has been given to the question of whether there are any convergence benefits for DPSGD, especially in the large batch setting.

In this paper, we find that DPSGD [33] greatly improves large batch training performance, as illustrated by the green curves in Figure 1. Since DPSGD only uses a partial average of neighboring learners' weights, each learner's weights differ from the weights of other learners. The differing weights between learners are an additional source of noise in DPSGD training. The key difference between SSGD, SSGD with Gaussian noise (denoted as "SSGD*" in this paper) and DPSGD is the source of noise during the update, and this noise directly affects performance in deep learning. This naturally motivates us to ask *Why does decentralized training outperform synchronous training in the large batch setting?* More specifically, we try to understand whether these performance differences are caused by differences in noise. We answer this question from both theoretical and empirical perspectives. Our contributions are:

- We analyze the dynamics of DDL algorithms, including both SSGD and DPSGD. We show, both theoretically and empirically, that the *intrinsic noise* in DPSGD automatically adjusts the effective learning rate when the batch size is large to help convergence. Note that the intrinsic noise comes completely for free in the DPSGD algorithm, and we show that it has a loss-landscape smoothing effect. Guided by our theoretical results, we also investigate training tasks where careful learning rate warmup schemes are required (e.g., Transformer models) [56, 42, 52] and find that DPSGD can work with a much shorter learning rate warmup period thus simplifying hyper-parameter tuning.

- We conduct extensive empirical studies of 18 CV, ASR, and NLP tasks with state-of-the-art CNN, LSTM, and Transformer models. Our experimental results demonstrate that DPSGD consistently outperforms SSGD, across application domains and Neural Network (NN) architectures in the large batch setting, *without any hyper-parameter tuning*. To the best of our knowledge, DPSGD is the only generic algorithm that can improve SSGD large batch training and shorten learning rate warmup period for this many models/tasks. Furthermore, unlike other solutions, DPSGD does not require global synchronization.

The remainder of this paper is organized as follows. Section 2 details the problem formulation and learning dynamics analysis of SSGD, SSGD*, and DPSGD; Section 3 and Section 4 detail the empirical results; Section 5 discusses related work; and Section 6 concludes the paper.

2 Analysis of stochastic learning dynamics in SSGD and DPSGD

We first formulate the dynamics of an SGD based learning algorithm with multiple ($n > 1$) learners indexed by $j = 1, 2, 3, ...n$ following the same theoretical framework established for a single learner [3]. At time (iteration) t, each learner has its own weight vector $\vec{w}_j(t)$, and the average weight vector $\vec{w}_a(t)$ is defined as: $\vec{w}_a(t) \equiv n^{-1}\sum_{j=1}^{n}\vec{w}_j(t)$. Each learner j updates its weight vector according to the cross-entropy loss function $L^{\mu_j(t)}(\vec{w})$ for minibatch $\mu_j(t)$ that is assigned to it at time t. The size of the local minibatch is B, and the overall batch size for all learners is nB. Two multi-learner algorithms, SSGD and DPSGD, are described below.

(1) Synchronous Stochastic Gradient Descent (SSGD): In the synchronous algorithm, each learner $j \in [1, n]$ starts from the average weight vector $\vec{w}_a$ and moves along the gradient of its local loss function $L^{\mu_j(t)}$ evaluated at the average weight $\vec{w}_a$:

$$\vec{w}_j(t+1) = \vec{w}_a(t) - \alpha\nabla L^{\mu_j(t)}(\vec{w}_a(t)), \tag{1}$$

where α is the learning rate.

(2) Decentralized Parallel SGD (DPSGD): In the DPSGD algorithm [33], each learner j computes the gradient at its own local weight $\vec{w}_j(t)$. The learning dynamics follows:

$$\vec{w}_j(t+1) = \vec{w}_{s,j}(t) - \alpha\nabla L^{\mu_j(t)}(\vec{w}_j(t)). \tag{2}$$

where $\vec{w}_{s,j}(t)$ is the starting weight set to be the average weight of a subset of "neighboring" learners of learner-j, which corresponds to the non-zero entries in the mixing matrix [2] defined in [33] (note that $\vec{w}_{s,j} = \vec{w}_a$ if all learners are included as neighbors).

By averaging over all learners, the learning dynamics for the average weight $\vec{w}_a$ for both SSGD and DPSGD can be written formally the same way as:

$$\vec{w}_a(t+1) = \vec{w}_a(t) - \alpha\vec{g}_a, \tag{3}$$

where $\vec{g}_a = n^{-1}\sum_{j=1}^{n}\vec{g}_j$ is the average gradient and $\vec{g}_j$ is the gradient from learner-j. The difference between SSGD and DPSGD is the weight at which $\vec{g}_j$ is computed: $\vec{g}_j \equiv \nabla L^{\mu_j(t)}(\vec{w}_a(t))$ is computed at $\vec{w}_a$ for SSGD; $\vec{g}_j \equiv \nabla L^{\mu_j(t)}(\vec{w}_j(t))$ is computed at $\vec{w}_j$ for DPSGD. The deviation of the weight for learner-j from the average weight is defined as $\delta\vec{w}_j \equiv \vec{w}_j - \vec{w}_a$. It is easy to see that $\delta\vec{w}_j(t+1) = \vec{w}_{s,j}(t) - \vec{w}_a(t) - \alpha[\vec{g}_j(t) - \vec{g}_a(t)]$, which depends on gradients at different points on the loss landscape.

2.1 Understanding DPSGD from the Optimization Perspective

The main difference between DPSGD and SSGD is that the stochastic gradients are calculated at different weights in DPSGD, while SSGD's stochastic gradient is calculated at the same weight. Intuitively, DPSGD explores more space than SSGD, which may help explain the empirical success of DPSGD. We formalize this intuition into the following theorem, which shows that DPSGD is optimizing a smoother landscape than SSGD.

[2] This is also called the "gossip matrix" in the literature, e.g., [27].

Theorem 1. *Denote $\mathcal{F}_t$ by the filtration generated by all the random variables until the t-th iteration. Suppose n is large enough that $\left\| \frac{1}{n}\sum_{i=1}^{n} \nabla L^{\mu_i(t)}(\vec{w}_i(t)) - \frac{1}{n-1}\sum_{i=1}^{n-1} \nabla L^{\mu_i(t)}(\vec{w}_i(t)) \right\| \leq \epsilon$ almost surely, and assume $\delta\vec{w}_i(t)|\mathcal{F}_{t-1} \overset{i.i.d.}{\sim} \mathcal{N}(0, \sigma_w^2 I)$ with $i = 1, \ldots, n-1$. Then from the $(t-1)$-th iteration to t-th iteration, SSGD and DPSGD are doing one step of stochastic gradient descent on two different functions $L(\vec{w})$ and $\tilde{L}(\vec{w}) \equiv \mathbb{E}_{\delta\vec{w}_i(t)}\left[L(\vec{w} + \delta\vec{w}_i(t)) \,|\, \mathcal{F}_{t-1}\right]$, respectively. The DPSGD loss $\tilde{L}(\vec{w})$ is smoother than the SSGD loss $L(\vec{w})$ if $L(\vec{w})$ is Lipschitz continuous.*

Remark: The proof of Theorem 1 can be found in Appendix A. Here, we briefly mention its implications. A function f is defined as l_s-smooth if $\|\nabla f(x) - \nabla f(y)\| \leq l_s\|x - y\|$ for any x, y, where l_s is the smoothness parameter of f. The landscape of the function f is smoother when l_s is smaller. Assume $L(\vec{w})$ is G-Lipschitz continuous, i.e., $|L(\vec{w}) - L(\vec{v})| \leq G\|\vec{w} - \vec{v}\|$, then by using Lemma 2 of [39], we know that the DPSGD landscape $\tilde{L}(\vec{w})$ is $\frac{2G}{\sigma_w}$-smooth. According to the convergence theory of SGD and DPSGD for nonconvex functions [11, 33, 12], the largest learning rate one can choose to guarantee convergence is $\frac{1}{l_s}$. For SSGD with the original loss landscape L, l_s can be very large (even close to $+\infty$ due to the nonsmooth nature of the ReLU activation) while l_s of the smoothed loss function $\tilde{L}$ for DPSGD is much smaller. This explains why we can use a larger learning rate in DPSGD as the landscape DPSGD sees has a smaller gradient-Lipschitz constant l_s than that in SSGD.

It is important to note that l_s of the smoothed loss function $\tilde{L}$ in DPSGD depends on the standard deviation σ_w of weights from different learners. Since σ_w depends on the loss landscape and changes with time (see Fig. 2(b)), the smoothing effect in DPSGD is self-adjusting – it is strong in the initial stage of training when the loss landscape is rough and becomes weaker as training progresses when the loss landscape becomes smoother. Our theoretical result suggests that this self-adjusting smoothing effect is responsible for DPSGD's convergence with a large learning rate in the large batch size setting. Next, we elaborate on this insight and verify it in a simple network for classification using the MNIST dataset.

Note that the Theorem 1 is only a one-step analysis. People may be interested in extending the analysis to trajectory-based analysis. We provide a sketch here. If we consider the perturbed objective $\tilde{L}(w) = \mathbb{E}_\delta\left[L(w + \delta)\right]$, where δ comes from the intrinsic noise of DPSGD, then we can utilize the descent lemma as shown in [11] to prove that DPSGD can converge to a stationary point of $\tilde{L}(w)$ in polynomial time. However, without the inherent noise of DPSGD, the landscape is rough and that is the reason why SSGD diverges. SSGD may not be able to converge to the stationary point of $L(w)$ (since the large learning rate in large batch setting makes the descent lemma not applicable in this case) or $\tilde{L}(w)$ (since there is no noise and landscape-smoothing effect in SSGD, so SSGD does not optimize the smoothed landscape). This is also consistent with our empirical evidence.

2.2 DPSGD Introduces a Landscape-Dependent Self-Adjusting Learning Rate that Helps Convergence

To understand the implication of the smoothing effect in DPSGD (Theorem 1) for learning dynamics, we define an effective learning rate $\alpha_e \equiv \alpha\vec{g}_a \cdot \vec{g}/||\vec{g}||^2$ by projecting the weight displacement vector $\Delta\vec{w}_a \equiv \alpha\vec{g}_a$ onto the direction of the gradient $\vec{g} \equiv \nabla L(\vec{w}_a)$ of the original loss function L at $\vec{w}_a$. The learning dynamics, Eq. 3, can be rewritten as:

$$\vec{w}_a(t+1) = \vec{w}_a(t) - \alpha_e\vec{g} + \vec{\eta}_\perp, \tag{4}$$

where the "noise" term $\vec{\eta}_\perp \equiv -\alpha\vec{g}_a + \alpha_e\vec{g}$ describes the random weight dynamics in directions orthogonal to $\vec{g}$. The noise term has zero mean $\langle\vec{\eta}_\perp\rangle_\mu = 0$ and the noise strength is characterized by its variance $\Delta(t) \equiv ||\vec{\eta}_\perp||^2$.

The effective learning rate α_e is related to the noise strength: $\alpha_e^2 = (\alpha^2||\vec{g}_a||^2 - \Delta)/||\vec{g}||^2$, which indicates that a higher noise strength Δ leads to a lower effective learning rate α_e. The DPSGD noise Δ_{DP} is larger than the SSGD noise Δ_S by an additional noise term $\Delta^{(2)}(>0)$ that originates from the difference of local weights $(\vec{w}_j)$ from their mean $(\vec{w}_a)$: $\Delta_{DP} = \Delta_S + \Delta^{(2)}$, see Appendix B for details. By expanding $\Delta^{(2)}$ w.r.t. $\delta\vec{w}_j$, we obtain the average $\Delta^{(2)}$ over minibatch ensemble $\{\mu\}$:

$$\begin{aligned}\langle\Delta^{(2)}\rangle_\mu &\equiv \alpha^2\langle||n^{-1}\sum_{j=1}^{n}[\nabla L^{\mu_j}(\vec{w}_j)-\nabla L^{\mu_j}(\vec{w}_a)]||^2\rangle_\mu \\ &\approx \alpha^2\sum_{k,l,l'}H_{kl}H_{kl'}C_{ll'},\end{aligned} \tag{5}$$

where $H_{kl}=\nabla^2_{kl}L$ is the Hessian matrix of the loss function and $C_{ll'}=n^{-2}\sum_{j=1}^{n}\delta w_{j,l}\delta w_{j,l'}$ is the weight covariance matrix. From Eq. 5 and the dependence of α_e on Δ, it is clear that the effective learning rate in DPSGD depends directly on the loss landscape (H) and indirectly via the weight variance, $\sigma_w^2=Tr(C)$, which decreases as the loss landscape becomes smooth (see Fig. 2(b)).

It is important to stress that the noise $\vec{\eta}_\perp$ in Eq.4 is not an artificially added noise. It is intrinsic to the use of minibatches (random subsampling) in all SGD-based algorithms (including SSGD and DPSGD). The noise is increased in DPSGD due to the weight difference among different learners ($\delta\vec{w}_j$). The noise strength Δ varies in weight space via its dependence on the loss landscape, as explicitly shown in Eq. 5. However, besides its landscape dependence, SGD noise scales inversely with the minibatch size B [3]. With n synchronized learners, the noise in SSGD scales as $1/(nB)$, which is too small to be effective for a large batch size nB. A main finding of our paper is that the additional landscape-dependent noise $\Delta^{(2)}$ in DPSGD can make up for the small SSGD noise when nB is large and help enhance convergence in the large batch setting.

The landscape dependent smoothing effect in DPSGD (shown in Sec. 2.1) indicates that α_e in DPSGD is reduced at the beginning of training when the landscape is rough. To demonstrate effects of the landscape-dependent self-adjusting learning rates, we did detailed analysis in numerical experiments using the MNIST dataset. In this experiment, we used $n=5$ learners with each learner a fully connected network with two hidden layers (50 units per layer) and we used $\vec{w}_{s,j}=\vec{w}_a$ for DPSGD. We focused on the large batch setting using $nB=2000$ and a large learning rate $\alpha=1$. As shown in Fig. 2(a), DPSGD converges to a solution with a low loss (2.1% test error), but SSGD fails to converge.

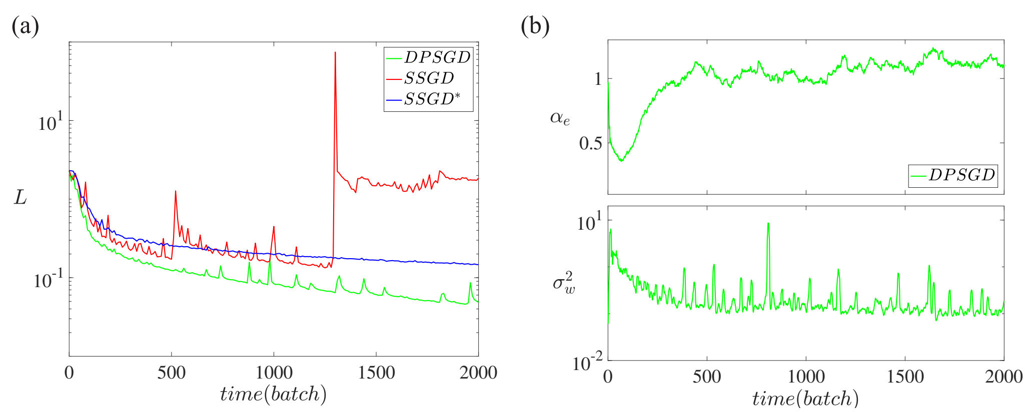

Figure 2: (a) Comparison of different multi-learner algorithms, DPSGD (green), SSGD (red), and SSGD* (blue) for a large learning rate $\alpha=1$. The adaptive learning rate allows DPSGD to converge while SSGD fails to converge. A fine-tuned SSGD* also converges but to an inferior solution. (b) The effective learning rate for DPSGD $\alpha_e(DPSGD)$ is self-adaptive to the landscape – it is reduced in the beginning of training when gradients are large and recovers to $\sim\alpha$ when the gradients are small. The weight variance $\sigma_w^2(t)$ has the opposite landscape-dependence as α_e and decreases with training time.

To understand the convergence in DPSGD, we computed the effective learning rate (α_e) and the weight variance (σ_w^2) during training. As shown in Fig. 2(b) (upper panel), the effective learning rate α_e is reduced in DPSGD during early training ($0\le t\le 700$). This reduction of α_e is caused by the stronger noise $\Delta^{(2)}$ in DPSGD (see Fig. 4 in Appendix B), which is essential for convergence when gradients are large in the beginning of the training process. In the later stage of the training process when gradients are smaller, the landscape-dependent DPSGD noise decreases and α_e *automatically* increases back to be $\approx\alpha$ to allow fast convergence. From Eq. 5, the landscape-dependent noise in

		AlexNet	VGG	VGG-BN
bs=256	Baseline	56.31/79.05	69.02/88.66	70.65/89.92
lr=1x		lr=0.01		lr=0.1
bs=2048	SSGD	**54.29/77.43**	**67.67/87.91**	**70.36/89.58**
lr=8x	DPSGD	53.71/76.91	67.28/87.58	69.76/89.31
bs=4096	SSGD	0.10/0.50	0.10/0.50	65.39/86.51
lr=16x	DPSGD	**52.53/76.01**	**66.44/87.20**	**68.86/88.82**
bs=8192	SSGD	0.10/0.50	0.10/0.50	0.10/0.50
lr=32x	DPSGD	**49.01/73.00**	**65.00/86.11**	**63.55/85.43**

Table 1: ImageNet-1K Top-1/Top-5 model accuracy (%) comparison for batch size 2048, 4096 and 8192. All experiments are conducted on 16 GPUs (learners), with batch size per GPU 128, 256 and 512 respectively. Bold text represents the best model accuracy achieved given the specific batch size and learning rate. The batch size 256 baseline is presented for reference. bs stands for batch-size, lr stands for learning rate. Baseline lr is set to 0.01 for AlexNet and VGG11, 0.1 for the other models. In the large batch setting, we use learning rate warmup and linear scaling as prescribed in [12]. For rough loss landscape like AlexNet and VGG, SSGD diverges when batch size is large whereas DPSGD converges.

DPSGD depends on the weight variance. As shown in Fig. 2(b) (lower panel), the weight variance σ_w^2 has a time-dependent trend that is opposite to α_e: σ_w^2 is large in the beginning of training when the landscape is rough and decreases as training progresses and the landscape becomes smoother.

To show the importance of the landscape-dependent weight variance, we used SSGD*, which injects a Gaussian noise with a constant variance to weights in SSGD, i.e., by setting $\delta\vec{w}_j \overset{i.i.d.}{\sim} \mathcal{N}(0, \sigma_0^2 I)$ with a constant σ_0^2. We found that SSGD* fails to converge for most choices of noise strength σ_0^2. Only by fine tuning σ_0^2 can SSGD* converge, but to an inferior solution with much higher loss and test error (5.7%) as shown in Fig. 2(a).

Finally, in addition to helping convergence, we found that the landscape-dependent noise in DPSGD can also help find flat minima with better generalization in the large batch setting (see Appendix C for details).

3 Experimental Methodology

We implemented SSGD and DPSGD using PyTorch, OpenMPI, and NVidia NCCL. We ran experiments on a cluster of two 8-V100-GPU x86 servers. For CV tasks, we evaluated on CIFAR-10 (50,000 training samples, 178MB) and ImageNet-1K (1.2 million training samples, 140GB). For ASR tasks, we evaluated on SWB-300 (300 hours training data, 4,000,000 samples, 30GB) and SWB-2000 (2000 hours training data, 30,000,000 samples, 216GB). For the NLP task, we evaluated on Wikitext-103(103 million tokens, 180MB). In all, we evaluate 18 state-of-the-art NN models: 15 CNN models, 2 6-layer bi-directional LSTM models, and 1 16-layer GPT-2 transformer model. We summarize the model sizes and training times in Table 6 of Appendix D. Also refer to Appendix D for hardware configuration, software implementation, dataset and Neural Network (NN) model details.

4 Experimental Results

All the large batch experiments are conducted on 16 GPUs (learners). Batches are evenly distributed among learners, e.g., with sixteen learners, each learner uses a local batch size that is one sixteenth the overall batch size. A learner randomly picks a neighbor with which to exchange weights in each DPSGD iteration [59].

4.1 SSGD and DPSGD Comparison on CV Tasks (CIFAR-10 and ImageNet-1K)

On ImageNet-1K we test 6 CNN models – AlexNet, VGG11, VGG11-BN, ResNet-50, ResNext-50 and DenseNet-161. Among them, AlexNet and VGG have rougher loss landscapes and can only work with smaller learning rates, while VGG11-BN, ResNet-50, ResNext-50, and DenseNet-161 have smoother loss landscapes thanks to the use of BatchNorm or Residual Connections, and thus can work with larger learning rates. We use the same baseline training recipe prescribed in [4]:

	SWB-300		
	bs2048	bs4096	bs8192
SSGD	1.58	10.37	10.37
DPSGD	1.59	1.60	1.66
	SWB-2000		
	bs2048	bs4096	bs8192
SSGD	1.46	1.46	10.37
DPSGD	1.45	1.47	1.47

Table 2: Heldout loss comparison for SSGD and DPSGD, evaluated on SWB-300 and SWB-2000. There are 32000 classes in this task, a held-out loss 10.37 (i.e. ln^{32000}) indicates a complete divergence. bs stands for batch size.

Figure 3: SSGD diverges when the learning rate warmup period is 75 iterations while DPSGD converges with a warmup period as short as 25 iterations. (Wikitext103, GPT-2)

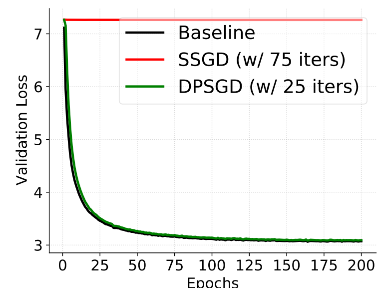

batch size 256, initial learning rate 0.01 for AlexNet and VGG-11 and 0.1 for the other 4 models, learning rate anneals by 0.1 every 30 epochs, 100 epochs in total. To study the model performance in the large batch setting, we follow the large batch size learning rate schedule prescribed in [12]: learning rate warmup for the first 5 epochs and then learning rate linear scaling w.r.t batch size. For example, in the AlexNet batch-size 8192 experiment, the learning rate is gradually warmed-up from 0.01 to 0.32 in the first 5 epochs, annealed to 0.032 from epoch 31 to epoch 60, annealed to 0.0032 from epoch 61 to epoch 90, and annealed to 0.00032 from epoch 91 to epoch 100. SSGD and DPSGD achieve comparable model accuracy in the large batch setting (see Table 10 in Appendix E.6). Most noticeably, when batch-size increases to 8192, SSGD diverges with AlexNet, VGG11, and VGG11-BN whereas DPSGD converges as shown in Table 1. Figure 9 in Appendix E.6 details the model accuracy progression versus epochs in each setting. Please see our detailed analysis of DPSGD vs SSGD on CIFAR-10 tasks throughout Appendix E.1 to Appendix E.5 where we document the DPSGD and SSGD comparison and loss landscape visualization (contour 2D projection and Hessian 2D projection), which show that DPSGD usually leads to much flatter optima than SSGD, and thus better generalization in the large batch setting.

Summary For rough loss landscapes like AlexNet and VGG, DPSGD converges whereas SSGD diverges in the large batch setting.

4.2 SSGD and DPSGD Comparison on ASR tasks

Unlike CV tasks where CNNs and their residual connection variants are the dominant models, ASR tasks overwhelmingly adopt RNN/LSTM models that capture sequence features. Furthermore, BatchNorm is known not to work well in RNN/LSTM tasks [31]. Finally, there are over 32,000 different classes with wildy uneven distribution in our ASR tasks due to the Zipfian characteristics of natural language. All in all, ASR tasks present a much more challenging loss landscape than CV tasks to optimize over.

For the SWB-300 and SWB-2000 tasks, we follow the same learning rate schedule proposed in [57]: we use learning rate 0.1 for baseline batch size 256, and linearly warmup the learning rate w.r.t the baseline batch size for the first 10 epochs before annealing the learning rate by $\frac{1}{\sqrt{2}}$ for the remaining 10 epochs. For example, when using a batch size 2048, we linearly warmup the learning rate to 0.8 by the end of the 10th epoch before annealing. Table 2 illustrates heldout loss for SWB-300 and SWB-2000. In the SWB-300 task, SSGD diverges beyond batch size 2048 and DPSGD converges well until batch size 8192. In the SWB-2000 task, SSGD diverges beyond batch size 4096 and DPSGD converges well until batch size 8192. Figure 10 in Appendix E.7 details the heldout loss progression versus epochs.

Summary For ASR tasks, SSGD diverges whereas DPSGD converges to baseline model accuracy in the large batch setting.

4.3 Noise-injection and Learning Rate Tuning

In 6 out of 17 studied CV and ASR tasks, a large batch setting leads to a complete divergence in SSGD: EfficientNet-B0, AlexNet, VGG11, VGG11-BN, SWB-300 and SWB-2000. As discussed in

		AlexNet	VGG11	VGG11-BN
lr*=32x	SSGD	0.10/0.50	0.10/0.50	0.10/0.50
	DPSGD	49.010/73.00	**65.004/86.11**	63.546/85.43
lr=16x	SSGD	0.10/0.50	0.10/0.50	**70.11/89.47**
	DPSGD	**49.26/73.14**	62.046/83.98	69.108/89.07
lr=8x	SSGD	46.40/70.25	45.32/70.61	69.54/89.22
	DPSGD	47.78/71.89	56.52/79.92	68.98/88.78
lr=4x	SSGD	41.77/66.44	50.20/74.83	68.61/88.57
	DPSGD	42.18/66.96	48.52/73.33	67.98/88.22

Table 3: ImageNet-1K learning rate tuning for AlexNet VGG11, VGG11-BN with batch-size 8192. Bold text in each column indicates the best top-1/top-5 accuracy achieved across different learning rate and optimization method configurations for the corresponding batch size. DPSGD consistently delivers the most accurate models. *The learning rate 1x used here corresponds to batch size 256 baseline learning rate, and we still adopt the same learning rate warmup, scaling and annealing schedule. Thus 32x refers to linear learning rate scaling when batch size is 8192. By reducing learning rate to 16x, 8x and 4x, SSGD can escape early traps but still lags behind compared to DPSGD in most cases.

		SWB-300 (bs4096)	SWB-300 (bs8192)	SWB-2000 (bs 8192)
lr*=1.6/3.2	SSGD	10.37	10.37	10.37
	DPSGD	**1.60**	**1.66**	**1.47**
lr=0.8/1.6	SSGD	10.37	10.37	10.37
	DPSGD	1.65	1.73	1.48
lr=0.4/0.8	SSGD	1.76	10.37	1.51
	DPSGD	1.77	1.80	1.52
lr=0.2/0.4	SSGD	1.92	2.05	1.58
	DPSGD	1.94	2.00	1.59

Table 4: Decreasing learning rate for SWB-300 and SWB-2000 (bs stands for batch-size). Bold text in each column indicates the best held-out loss achieved across different learning rate and optimization method configurations for the corresponding batch size. DPSGD consistently delivers the most accurate models. *learning rate 1.6 is used for bs4096 and learning rate 3.2 is used for bs8192. We still adopt the same learning rate warmup, scaling and annealing schedule (baseline learning rate is 0.1 for batch size 256).

Section 2, the intrinsic landscape-dependent noise in DPSGD effectively helps escape early traps (e.g., saddle points) and improves training by automatically adjusting the learning rate. In this section, we demonstrate these facts by systematically adding Gaussian noise (the same as the $SSGD^*$ algorithm in Section 2) and decreasing the learning rate. We find that SSGD might escape early traps but still results in a much inferior model compared to DPSGD.

Noise-injection In Figure 1, we systematically explore Gaussian noise injection with mean 0 and standard deviation (std) ranging from 10 to 0.00001 via binary search (i.e. roughly 20 configurations for each task). We found in the vast majority of the setups, noise-injection cannot escape early traps. In EfficientNet-B0, only when std is set to 0.04, does the model start to converge, but to a very low accuracy (test accuracy 22.15% in SSGD vs 91.13% in DPSGD). In the SWB-300 case, when std is 0.01, SSGD shows an early sign of converging for the first 3 epochs before it starts to diverge. In the AlexNet, VGG11, VGG11-BN, and SWB-2000 cases, we didn't find any configuration that can escape early traps. Figure 1 characterizes our best-effort Gaussian noise tuning and its comparison against SSGD and DPSGD. A plausible explanation is that Gaussian noise injection escapes saddle points very slowly, since Gaussian noise is isotropic and the complexity for finding local minima is dimension-dependent [10]. Deep Neural Networks are usually over-parameterized (i.e., high-dimensional), so it may take a long time to escape local traps. In contrast, the heightened landscape-dependent noise in DPSGD is anisotropic [3, 8] and can drive the system to escape in the right directions.

Learning Rate Tuning To make otherwise-divergent SSGD training converge in the large batch setting, we systematically tune down the learning rates. Table 3 and Table 4 compare the model quality trained by SSGD and DPSGD using smaller learning rates in the large batch setting, for ImageNet and

ASR tasks. Table 9 in Appendix E.3 illustrates the similar learning rate tuning effort for CIFAR-10 tasks. As we can see, by using a smaller learning rate, SSGD can escape early traps and converge, however it consistently lags behind DPSGD in the large batch setting. Morever, DPSGD does not depend on such an exhaustive learning rate tuning to achieve convergence. DPSGD can simply follow the learning rate warm-up and linear scaling rules [12] whereas SSGD requires much more stringent learning rate tuning. This implies DPSGD practitioners enjoy a much larger degree of freedom when it comes to hyper-parameter tuning in the large batch setting than the SSGD practitioners.

Summary By systematically introducing landscape-independent noise and reducing the learning rate, SSGD could escape early traps (e.g., saddle points), but results in much inferior models compared to DPSGD in the large batch setting.

4.4 DPSGD and SSGD Runtime Comparison

In Appendix F, we detail runtime comparison between DPSGD and SSGD and demonstrate DPSGD consistently runs faster than SSGD. We also compare DPSGD with LAMB[55], a state-of-the-art optimizer specifically designed for synchronous large-batch training, demonstrating that DPSGD can avoid straggler problems in distributed training.

4.5 SSGD and DPSGD Comparison on NLP tasks (Wikitext-103)

For NLP tasks such as Masked Language Modeling (MLM) [6, 50], a careful learning rate warmup scheme needs to be designed so that learning rate grows from 0 to a desired learning rate gradually. Too short a warmup period often leads to divergence and practitioners need to restart training, which wastes huge computational resources[42, 52, 56]. We test our theory by finding the shortest viable learning rate warmup period for SSGD and DPSGD. We use the hyper-parameter settings prescribed in [52], warmup learning rate 0 to 2.5×10^{-4} in the first 64000 samples (i.e., 250 iterations of batch size 256) and then cosine-annealing to zero on top of an Adam optimizer. We then shorten the learning rate warmup period and check convergence. Figure 3 and Table 5 show that SSGD diverges when the learning rate warmup period is shorter than 100 iterations, while DPSGD converges with a warmup period as short as 25 iterations. Figure 1c shows that injecting independent random noise into SSGD (in the same fashion as Section 4.3) does not help SSGD escape early training traps. These experiments corroborate our theory that DPSGD can leverage loss landscape noise to self-adjust the learning rate.

Warmup(iters)	250	100	75	50	25	15
SYNC	3.09	3.07	7.26	7.26	7.26	7.26
DPSGD	3.08	3.053	3.06	3.08	3.09	7.26

Table 5: Validation loss comparison when shortening the learning rate warmup period. DPSGD can converge with a much shorter warmup. All experiments are conducted on 16 GPUs (learners). Wikitext-103, GPT-2 model, 200 epochs training in total.

5 Related Works

Please see Appendix G

6 Conclusion

In this paper, we find that in the large-batch and large-learning-rate setting, DPSGD yields comparable model accuracy when SSGD converges; moreover, DPSGD converges when SSGD diverges. We then investigate why DPSGD outperforms SSGD for large batch training. Through detailed analysis on small-scale tasks and an extensive empirical study of a diverse set of modern DL tasks, we conclude that the landscape-dependent noise, which is strengthened in the DPSGD system, self-adjusts the effective learning rate according to the loss landscape, helping convergence. This self-adjusting learning rate effect is a mere by-product of the inherent loss-landscape-dependent-noise of the DPSGD training algorithm and requires no additional computation, no additional communication and no additional hyper-parameter tuning. The theory was originally developed to understand why DPSGD outperforms SSGD in the large batch setting for CV and ASR tasks. The same theory can be also verified in NLP tasks where when a carefully designed learning rate warmup scheme is required.

References

[1] Carlo Baldassi, Christian Borgs, Jennifer T. Chayes, Alessandro Ingrosso, Carlo Lucibello, Luca Saglietti, and Riccardo Zecchina. Unreasonable effectiveness of learning neural networks: From accessible states and robust ensembles to basic algorithmic schemes. *Proceedings of the National Academy of Sciences*, 113(48):E7655–E7662, 2016.

[2] Pratik Chaudhari, Anna Choromanska, Stefano Soatto, Yann LeCun, Carlo Baldassi, Christian Borgs, Jennifer Chayes, Levent Sagun, and Riccardo Zecchina. Entropy-sgd: Biasing gradient descent into wide valleys, 2016.

[3] Pratik Chaudhari and Stefano Soatto. Stochastic gradient descent performs variational inference, converges to limit cycles for deep networks. *2018 Information Theory and Applications Workshop (ITA)*, Feb 2018.

[4] Soumith Chintala. *PyTorch ImageNet Examples*, 2020. Available at https://github.com/pytorch/examples/tree/master/imagenet.

[5] J. Deng, W. Dong, R. Socher, L. Li, Kai Li, and Li Fei-Fei. Imagenet: A large-scale hierarchical image database. In *2009 IEEE Conference on Computer Vision and Pattern Recognition*, pages 248–255, 2009.

[6] Jacob Devlin, Ming-Wei Chang, Kenton Lee, and Kristina Toutanova. BERT: Pre-training of deep bidirectional transformers for language understanding. In *Proceedings of the 2019 Conference of the North American Chapter of the Association for Computational Linguistics: Human Language Technologies, Volume 1 (Long and Short Papers)*, pages 4171–4186, Minneapolis, Minnesota, June 2019. Association for Computational Linguistics.

[7] Gintare Karolina Dziugaite and Daniel M Roy. Computing nonvacuous generalization bounds for deep (stochastic) neural networks with many more parameters than training data. *arXiv preprint arXiv:1703.11008*, 2017.

[8] Yu Feng and Yuhai Tu. The inverse variance–flatness relation in stochastic gradient descent is critical for finding flat minima. *Proceedings of the National Academy of Sciences*, 118(9), 2021.

[9] Pierre Foret, Ariel Kleiner, Hossein Mobahi, and Behnam Neyshabur. Sharpness-aware minimization for efficiently improving generalization. *ICLR*, 2021.

[10] Rong Ge, Furong Huang, Chi Jin, and Yang Yuan. Escaping from saddle points—online stochastic gradient for tensor decomposition. In *Conference on Learning Theory*, pages 797–842, 2015.

[11] Saeed Ghadimi and Guanghui Lan. Stochastic first-and zeroth-order methods for nonconvex stochastic programming. *SIAM Journal on Optimization*, 23(4):2341–2368, 2013.

[12] Priya Goyal, Piotr Dollár, Ross B. Girshick, Pieter Noordhuis, Lukasz Wesolowski, Aapo Kyrola, Andrew Tulloch, Yangqing Jia, and Kaiming He. Accurate, large minibatch SGD: training imagenet in 1 hour. *CoRR*, abs/1706.02677, 2017.

[13] Vipul Gupta, Santiago Akle Serrano, and Dennis DeCoste. Stochastic weight averaging in parallel: Large-batch training that generalizes well. *ICLR*, 2020.

[14] Kaiming He, Xiangyu Zhang, Shaoqing Ren, and Jian Sun. Deep residual learning for image recognition. *CVPR*, 2015.

[15] Geoffrey Hinton, Li Deng, Dong Yu, George Dahl, Abdel rahman Mohamed, Navdeep Jaitly, Andrew Senior, Vincent Vanhoucke, Patrick Nguyen, Tara Sainath, and Brian Kingsbury. Deep neural networks for acoustic modeling in speech recognition. *Signal Processing Magazine*, 2012.

[16] Geoffrey E. Hinton and Drew van Camp. Keeping the neural networks simple by minimizing the description length of the weights. In *Proceedings of the Sixth Annual Conference on Computational Learning Theory*, COLT '93, pages 5–13, New York, NY, USA, 1993. ACM.

[17] Sepp Hochreiter and Jürgen Schmidhuber. Flat minima. *Neural Computation*, 9(1):1–42, 1997.

[18] Elad Hoffer, Itay Hubara, and Daniel Soudry. Train longer, generalize better: closing the generalization gap in large batch training of neural networks. In *Advances in Neural Information Processing Systems*, pages 1731–1741, 2017.

[19] Andrew G. Howard, Menglong Zhu, Bo Chen, Dmitry Kalenichenko, Weijun Wang, Tobias Weyand, Marco Andreetto, and Hartwig Adam. Mobilenets: Efficient convolutional neural networks for mobile vision applications. *CoRR*, abs/1704.04861, 2017.

[20] G. Huang, Z. Liu, L. Van Der Maaten, and K. Q. Weinberger. Densely connected convolutional networks. In *2017 IEEE Conference on Computer Vision and Pattern Recognition (CVPR)*, pages 2261–2269, 2017.

[21] Sergey Ioffe and Christian Szegedy. Batch normalization: Accelerating deep network training by reducing internal covariate shift. *ICML*, 2015.

[22] Stanisław Jastrzębski, Zachary Kenton, Devansh Arpit, Nicolas Ballas, Asja Fischer, Yoshua Bengio, and Amos Storkey. Three factors influencing minima in sgd. *arXiv preprint arXiv:1711.04623*, 2017.

[23] Stanislaw Jastrzebski, Zachary Kenton, Devansh Arpit, Nicolas Ballas, Asja Fischer, Yoshua Bengio, and Amos J Storkey. Finding flatter minima with sgd. In *ICLR (Workshop)*, 2018.

[24] Nitish Shirish Keskar, Dheevatsa Mudigere, Jorge Nocedal, Mikhail Smelyanskiy, and Ping Tak Peter Tang. On large-batch training for deep learning: Generalization gap and sharp minima. *arXiv preprint arXiv:1609.04836*, 2016.

[25] D. P. Kingma and J. L. Ba. ADAM: a method for stochastic optimization. In *International Conference on Learning Representations (ICLR)*, 2015.

[26] Robert Kleinberg, Yuanzhi Li, and Yang Yuan. An alternative view: When does sgd escape local minima? *arXiv preprint arXiv:1802.06175*, 2018.

[27] Anastasia Koloskova, Sebastian Stich, and Martin Jaggi. Decentralized stochastic optimization and gossip algorithms with compressed communication. In *International Conference on Machine Learning*, pages 3478–3487. PMLR, 2019.

[28] Alex Krizhevsky and Geoffrey Hinton. Learning multiple layers of features from tiny images. *Computer Science Department, University of Toronto, Tech. Rep*, 1(4):7, 2009.

[29] Alex Krizhevsky, Ilya Sutskever, and Geoffrey E Hinton. Imagenet classification with deep convolutional neural networks. In *Advances in neural information processing systems*, pages 1097–1105, 2012.

[30] Sameer Kumar, Victor Bitorff, Dehao Chen, Chiachen Chou, Blake Hechtman, HyoukJoong Lee, Naveen Kumar, Peter Mattson, Shibo Wang, Tao Wang, Yuanzhong Xu, and Zongwei Zhou. Scale MLPerf-0.6 models on Google TPU-v3 Pods. *arXiv e-prints*, page arXiv:1909.09756, September 2019.

[31] César Laurent, Gabriel Pereyra, Philémon Brakel, Ying Zhang, and Yoshua Bengio. Batch normalized recurrent neural networks, 2016.

[32] Hao Li, Zheng Xu, Gavin Taylor, Christoph Studer, and Tom Goldstein. Visualizing the loss landscape of neural nets. In S. Bengio, H. Wallach, H. Larochelle, K. Grauman, N. Cesa-Bianchi, and R. Garnett, editors, *Advances in Neural Information Processing Systems 31*, pages 6389–6399. Curran Associates, Inc., 2018.

[33] Xiangru Lian, Ce Zhang, Huan Zhang, Cho-Jui Hsieh, Wei Zhang, and Ji Liu. Can decentralized algorithms outperform centralized algorithms? a case study for decentralized parallel stochastic gradient descent. In *Advances in Neural Information Processing Systems*, pages 5330–5340, 2017.

[34] Xiangru Lian, Wei Zhang, Ce Zhang, and Ji Liu. Asynchronous decentralized parallel stochastic gradient descent. In *ICML*, 2018.

[35] Tao Lin, Lingjing Kong, Sebastian Stich, and Martin Jaggi. Extrapolation for large-batch training in deep learning. In Hal Daumé III and Aarti Singh, editors, *Proceedings of the 37th International Conference on Machine Learning*, volume 119 of *Proceedings of Machine Learning Research*, pages 6094–6104. PMLR, 13–18 Jul 2020.

[36] Tao Lin, Sebastian U. Stich, and Martin Jaggi. Don't use large mini-batches, use local SGD. *ICLR*, 2020.

[37] Kang Liu. *Train CIFAR10 with PyTorch*, 2020. Available at https://github.com/kuangliu/pytorch-cifar.

[38] Stephen Merity, Caiming Xiong, James Bradbury, and Richard Socher. Pointer sentinel mixture models. *ICLR*, 2017.

[39] Yurii Nesterov and Vladimir Spokoiny. Random gradient-free minimization of convex functions. *Foundations of Computational Mathematics*, 17(2):527–566, 2017.

[40] Behnam Neyshabur, Srinadh Bhojanapalli, David McAllester, and Nati Srebro. Exploring generalization in deep learning. In *Advances in Neural Information Processing Systems*, pages 5947–5956, 2017.

[41] Behnam Neyshabur, Srinadh Bhojanapalli, and Nathan Srebro. A pac-bayesian approach to spectrally-normalized margin bounds for neural networks. *arXiv preprint arXiv:1707.09564*, 2017.

[42] Alec Radford, Karthik Narasimhan, Tim Salimans, and Ilya Sutskever. Improving language understanding by generative pre-training. 2018.

[43] Alec Radford, Jeff Wu, Rewon Child, David Luan, Dario Amodei, and Ilya Sutskever. Language models are unsupervised multitask learners. 2019.

[44] Sashank J. Reddi, Satyen Kale, and Sanjiv Kumar. On the convergence of adam and beyond. In *International Conference on Learning Representations*, 2018.

[45] Mark Sandler, Andrew G. Howard, Menglong Zhu, Andrey Zhmoginov, and Liang-Chieh Chen. Inverted residuals and linear bottlenecks: Mobile networks for classification, detection and segmentation. *CVPR*, abs/1801.04381, 2018.

[46] K. Simonyan and A. Zisserman. Very deep convolutional networks for large-scale image recognition. *International Conference on Learning Representations*, 2015.

[47] Samuel L Smith and Quoc V Le. A bayesian perspective on generalization and stochastic gradient descent. *arXiv preprint arXiv:1710.06451*, 2017.

[48] Christian Szegedy, Wei Liu, Yangqing Jia, Pierre Sermanet, Scott E. Reed, Dragomir Anguelov, Dumitru Erhan, Vincent Vanhoucke, and Andrew Rabinovich. Going deeper with convolutions. *CoRR*, abs/1409.4842, 2014.

[49] Mingxing Tan and Quoc V. Le. Efficientnet: Rethinking model scaling for convolutional neural networks. *ICML*, abs/1905.11946, 2019.

[50] Ashish Vaswani, Noam Shazeer, Niki Parmar, Jakob Uszkoreit, Llion Jones, Aidan N Gomez, Ł ukasz Kaiser, and Illia Polosukhin. Attention is all you need. In I. Guyon, U. V. Luxburg, S. Bengio, H. Wallach, R. Fergus, S. Vishwanathan, and R. Garnett, editors, *Advances in Neural Information Processing Systems 30*, pages 5998–6008. Curran Associates, Inc., 2017.

[51] Yeming Wen, Kevin Luk, Maxime Gazeau, Guodong Zhang, Harris Chan, and Jimmy Ba. An empirical study of stochastic gradient descent with structured covariance noise. In Silvia Chiappa and Roberto Calandra, editors, *Proceedings of the Twenty Third International Conference on Artificial Intelligence and Statistics*, volume 108 of *Proceedings of Machine Learning Research*, pages 3621–3631. PMLR, 26–28 Aug 2020.

[52] Thomas Wolf. *Transfer Learning in Natural Language Processing*, 2019. Available at https://github.com/huggingface/naacl_transfer_learning_tutorial.

[53] Saining Xie, Ross B. Girshick, Piotr Dollár, Zhuowen Tu, and Kaiming He. Aggregated residual transformations for deep neural networks. *CVPR*, abs/1611.05431, 2017.

[54] Yang You, Igor Gitman, and Boris Ginsburg. Scaling SGD batch size to 32k for imagenet training. *CoRR*, abs/1708.03888, 2017.

[55] Yang You, Jing Li, Jonathan Hseu, Xiaodan Song, James Demmel, and Cho-Jui Hsieh. Reducing BERT pre-training time from 3 days to 76 minutes. *CoRR*, abs/1904.00962, 2019.

[56] Susan Zhang, Stephen Roller, Naman Goyal, Mikel Artetxe, Moya Chen, Shuohui Chen, Christopher Dewan, Mona Diab, Xian Li, Xi Victoria Lin, Todor Mihaylov, Myle Ott, Sam Shleifer, Kurt Shuster, Daniel Simig, Punit Singh Koura, Anjali Sridhar, Tianlu Wang, and Luke Zettlemoyer. Opt: Open pre-trained transformer language models, 2022.

[57] Wei Zhang, Xiaodong Cui, Ulrich Finkler, Brian Kingsbury, George Saon, David Kung, and Michael Picheny. Distributed deep learning strategies for automatic speech recognition. In *ICASSP'2019*, May 2019.

[58] Wei Zhang, Xiaodong Cui, Ulrich Finkler, George Saon, Abdullah Kayi, Alper Buyuktosunoglu, Brian Kingsbury, David Kung, and Michael Picheny. A highly efficient distributed deep learning system for automatic speech recognition. In *INTERSPEECH'2019*, Sept 2019.

[59] Wei Zhang, Xiaodong Cui, Abdullah Kayi, Mingrui Liu, Ulrich Finkler, Brian Kingsbury, George Saon, Youssef Mroueh, Alper Buyuktosunoglu, Payel Das, David Kung, and Michael Picheny. Improving efficiency in large-scale decentralized distributed training. In *ICASSP'2020*, May 2020.

[60] Wei Zhang, Suyog Gupta, Xiangru Lian, and Ji Liu. Staleness-aware async-sgd for distributed deep learning. In *Proceedings of the Twenty-Fifth International Joint Conference on Artificial Intelligence, IJCAI 2016, New York, NY, USA, 9-15 July 2016*, pages 2350–2356, 2016.

[61] Wei Zhang, Suyog Gupta, and Fei Wang. Model accuracy and runtime tradeoff in distributed deep learning: A systematic study. In *IEEE International Conference on Data Mining*, 2016.

[62] Xiangyu Zhang, Xinyu Zhou, Mengxiao Lin, and Jian Sun. Shufflenet: An extremely efficient convolutional neural network for mobile devices. *CVPR*, abs/1707.01083, 2018.

[63] Yao Zhang, Andrew M. Saxe, Madhu S. Advani, and Alpha A. Lee. Energy–entropy competition and the effectiveness of stochastic gradient descent in machine learning. *Molecular Physics*, 116(21-22):3214–3223, Jun 2018.

[64] Fan Zhou and Guojing Cong. On the convergence properties of a k-step averaging stochastic gradient descent algorithm for nonconvex optimization. In *IJCAI-18*, pages 3219–3227, 7 2018.

Checklist

1. For all authors...
   (a) Do the main claims made in the abstract and introduction accurately reflect the paper's contributions and scope? [Yes]
   (b) Did you describe the limitations of your work? [Yes]
   (c) Did you discuss any potential negative societal impacts of your work? [N/A]
   (d) Have you read the ethics review guidelines and ensured that your paper conforms to them? [Yes]
2. If you are including theoretical results...
   (a) Did you state the full set of assumptions of all theoretical results? [Yes]
   (b) Did you include complete proofs of all theoretical results? [Yes]
3. If you ran experiments...
   (a) Did you include the code, data, and instructions needed to reproduce the main experimental results (either in the supplemental material or as a URL)? [Yes] Not code(proprietary), but enough instructions to reproduce the results.
   (b) Did you specify all the training details (e.g., data splits, hyperparameters, how they were chosen)? [Yes]
   (c) Did you report error bars (e.g., with respect to the random seed after running experiments multiple times)? [No]
   (d) Did you include the total amount of compute and the type of resources used (e.g., type of GPUs, internal cluster, or cloud provider)? [Yes]
4. If you are using existing assets (e.g., code, data, models) or curating/releasing new assets...
   (a) If your work uses existing assets, did you cite the creators? [Yes]
   (b) Did you mention the license of the assets? [N/A]
   (c) Did you include any new assets either in the supplemental material or as a URL? [No]
   (d) Did you discuss whether and how consent was obtained from people whose data you're using/curating? [N/A]
   (e) Did you discuss whether the data you are using/curating contains personally identifiable information or offensive content? [N/A]
5. If you used crowdsourcing or conducted research with human subjects...
   (a) Did you include the full text of instructions given to participants and screenshots, if applicable? [N/A]

(b) Did you describe any potential participant risks, with links to Institutional Review Board (IRB) approvals, if applicable? [N/A]

(c) Did you include the estimated hourly wage paid to participants and the total amount spent on participant compensation? [N/A]

A Proof of Theorem 1

We first start to compare the learning dynamics of DPSGD and SSGD respectively. For DPSGD, we have

$$\vec{w}_a(t+1) = \vec{w}_a(t) - \alpha \cdot \frac{1}{n}\sum_{i=1}^{n} \nabla L^{\mu_i(t)}(\vec{w}_i(t)), \tag{6}$$

where n is the number of machines, $i = 1, \ldots, n$ is the index of the machine, $\vec{w}_i(t)$ is the weight of the model at the t-th iteration on i-th machine, $\vec{w}_a(t) = \frac{1}{n}\sum_{i=1}^{n} \vec{w}_i(t)$, L is the loss function, $\mu_i(t)$ denotes the minibatch sampled from the i-th machine at the t-th iteration, and α is the learning rate. In contrast, SSGD's update rule is

$$\vec{w}_a(t+1) = \vec{w}_a(t) - \alpha \cdot \frac{1}{n}\sum_{i=1}^{n} \nabla L^{\mu_i(t)}(\vec{w}_a(t)). \tag{7}$$

Define $\delta\vec{w}_i(t) = \vec{w}_a(t) - \vec{w}_i(t)$. Let us consider following fact: Given the realization of $\mu_i(t-1)$, $\vec{w}_i(t)$'s are mutually independent, and any $n-1$ random variables selected from $\{\delta\vec{w}_i(t)\}_{i=1}^{n}$ are mutually independent due to $\sum_{i=1}^{n} \delta\vec{w}_i(t) = 0$.

When n is sufficiently large, we have the surrogate minibatch gradient with batch size $n-1$ ($\frac{1}{n-1}\sum_{i=1}^{n-1} \nabla L^{\mu_i(t)}(\vec{w}_i(t))$) to be ϵ-close to the minibatch gradient with size n ($\frac{1}{n}\sum_{i=1}^{n} \nabla L^{\mu_i(t)}(\vec{w}_i(t))$), and hence can be regarded as approximate minibatch gradient with batch size $n-1$, which are sampled i.i.d. from $\{\delta\vec{w}_i(t)\}_{i=1}^{n-1} \mid \mathcal{F}_{t-1}$. Once we have the independence, we can find that both (6) and (7) are doing SGD update, with different objective functions. In addition, assuming $\{\delta\vec{w}_i(t)\}_{i=1}^{n-1} \mid \mathcal{F}_{t-1}$ are i.i.d. Gaussian distribution is also reasonable due to the central limit theorem and the fact that n is sufficiently large.

Then at the t-th iteration, (6) is using one step of SGD to optimize $L(\vec{w})$ directly, while (7) is using one step of SGD to optimize a smoothed version of L, which is $\mathbb{E}_{\delta\vec{w}_i(t)}\left[L(\vec{w} + \delta\vec{w}_i(t)) \mid \mathcal{F}_{t-1}\right]$.

Suppose $L(\vec{w})$ is G-Lipschitz continuous, by using Lemma 2 of [39], we know that the landscape DPSGD is trying to optimize over is $\tilde{L}(\vec{w})$ is $\frac{2G}{\sigma_w}$-smooth.

B Appendix for the Noise Analysis

To understand the origin of the noise term $\vec{\eta}$ in DPSGD, we decompose the gradient $\vec{g}_j$ for an individual learner-j:

$$\begin{aligned} \vec{g}_j &= \vec{g}_0 + \delta g_j^{(1)} + \delta g_j^{(2)} \\ &= \nabla L^{\mu}(\vec{w}_a) + [\nabla L^{\mu_j}(\vec{w}_a) - \nabla L^{\mu}(\vec{w}_a)] \\ &+ [\nabla L^{\mu_j}(\vec{w}_j) - \nabla L^{\mu_j}(\vec{w}_a)], \end{aligned} \tag{8}$$

where the first term $\vec{g}_0 \equiv \nabla L^{\mu}(\vec{w}_a)$ in the right hand side of Eq. 8 is the gradient of the loss function over the "superbatch" μ defined as the sum of all the minibatches for different learners at a given iteration: $\mu(t) = \sum_{j=1}^{n} \mu_j(t)$; the second term $\delta g_j^{(1)} \equiv \nabla L^{\mu_j}(\vec{w}_a) - \nabla L^{\mu}(\vec{w}_a)$ describes the gradient difference (fluctuation) between a minibatch μ_j and the superbatch μ; the third term $\delta g_j^{(2)} \equiv \nabla L^{\mu_j}(\vec{w}_j) - \nabla L^{\mu_j}(\vec{w}_a)$ represents the difference (fluctuation) of the gradients at the individual weight $\vec{w}_j$ and at the average weight $\vec{w}_a$. Note that $\delta g_j^{(2)} = 0$ in SSGD as the gradients are taken at the average weight $\vec{w}_a$ for all learners. By taking the average of Eq. 8 over j, we have: $\vec{g}_a = \vec{g}_0 + \delta g_a^{(1)} + \delta g_a^{(2)}$ with $\delta g_a^{(i)} = n^{-1}\sum_{j=1}^{n} \delta g_j^{(i)}$ $(i = 1, 2)$. Here, $\delta g_a^{(1)}$ vanishes after averaging over all minibatch. $\delta g_a^{(0)}$ is due to superbatch-superbatch difference and $\delta g_a^{(2)}$ comes from weight-weight difference in DPSGD. The gradient fluctuation has zero mean and its variance given by: $\Delta^{(2)} \equiv \alpha^2 ||\delta\vec{g}_a^{(2)}||^2$. Finally, the noise strength in DPSGD Δ_{DP} can be expressed as:

$$\Delta_{DP} \equiv ||\vec{\eta}||^2 = \Delta_S + \Delta^{(2)}, \tag{9}$$

where $\Delta_S \equiv \alpha^2(||\vec{g}_0||^2 - (\vec{g}_0 \cdot \vec{g})^2/||\vec{g}||^2)$ is the SSGD noise strength which is equivalent to the noise strength in a single-learner SGD algorithm with a superbatch (size nB). The $\Delta^{(2)}$ term only exists in DPSGD. In general, this additional contribution makes the learning noise larger in DPSGD than that in SSGD, although noise strength also depends on $\vec{g_a}$, $\vec{g}_0$, etc., which may be different for different algorithms.

In Fig. 4, we calculated these two noise components of DPSGD for the experiment shown in Fig. 2. Due to the large batch size we used in the experiment, Δ_S is very small during the training process. However, the additional landscape-dependent noise $\Delta^{(2)}$ in DPSGD can make up for the small SSGD noise when nB is large and adaptively adjust the effectively learning rate α_e according to the loss landscape to help convergence. This additional landscape dependent noise in SGD is also responsible for finding flat minima with good generalization performance as shown in Fig. 5 in Appendix C.

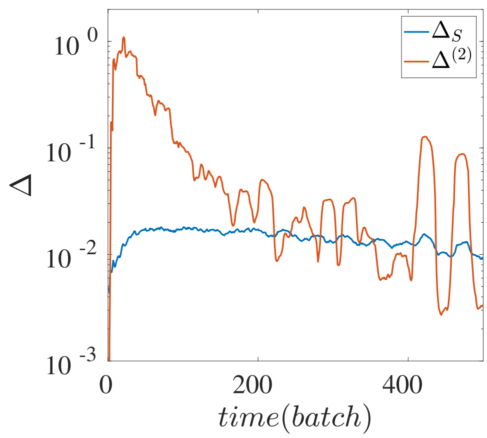

Figure 4: The noise in DPSGD can be decomposed into the SSGD noise Δ_S evaluated at the mean weight $\vec{w}_a$ plus an additional noise $\Delta^{(2)}(> 0)$. The additional DPSGD noise $\Delta^{(2)} \gg \Delta_S$ in the beginning of the training before it decreases to become comparable to Δ_S.

C Appendix for the effect of DPSGD noise in help finding flat minima with better generalization

To demonstrate the effect of the additional noise in DPSGD for finding flat minima, we consider a numerical experiment with a smaller learning rate $\alpha = 0.2$ for the MNIST dataset. We used $n = 6$ and $\vec{w}_{s,j}(t)$ in DPSGD is the average weight of 2 neighbors on each side. In this case, both SSGD and DPSGD can converge to a solution, but their learning dynamics are different. As shown in Fig. 5 (upper panel), while the training loss L of SSGD (red) decreases smoothly, the DPSGD training loss (green) fluctuates widely during the time window (1000-3000) when it stays significantly above the SSGD training loss. As shown in Fig. 5 (lower panel), these large fluctuations in L are caused by the high and increasing noise level in DPSGD. This elevated noise level in DPSGD allows the algorithm to search in a wider region in weight space. At around time 3000(batch), the DPSGD loss decreases suddenly and eventually converges to a solution with a similar training loss as SSGD. However, despite their similar final training loss, the DPSGD loss landscape is flatter (contour lines further apart) than SSGD landscape. Remarkably, the DPSGD solution has a lower test error (2.3$\%$) than the test error of the SSGD solution (2.6$\%$). We have also tried the SSGD* algorithm, but the performance (3.9$\%$ test error) is worse than both $SSGD$ and $DPSGD$.

To understand their different generalization performance, we studied the loss function landscape around the SSGD and DPSGD solutions. The contour plots of the loss function L around the two solutions are shown in the two right panels in Fig. 5. We found that the loss landscape near the DPSGD solution is flatter than the landscape near the SSGD solution despite having the same minimum loss. Our observation is consistent with [24] where it was found that SSGD with a large batch size converges to a sharp minimum which does not generalize well. Our results are in general agreement with the current consensus that flatter minima have better generalization [16, 17, 1, 2, 63]. It was recently suggested that the landscape-dependent noise in SGD-based algorithms can drive the system towards flat minima [8]. However, in the large batch setting, the SSGD noise is too small to be

	WikiText-103	CIFAR10				
	GPT-2	EfficientNet-B0	VGG-19	ResNet-18	DenseNet-121	MobileNet
Size	201.58MB	11.11 MB	76.45 MB	42.63 MB	26.54 MB	12.27 MB
Time	320Hr	2.92 Hr	1.08 Hr	1.37 Hr	5.48 Hr	1.02 Hr
	CIFAR10				SWB300	SWB2000
	MobileNetV2	ShuffleNet	GoogleNet	ResNext-29	LSTM	LSTM
Size	8.76 MB	4.82 MB	23.53 MB	34.82 MB	164.62 MB	164.62 MB
Time	1.96 Hr	2.46 Hr	5.31 Hr	4.55 Hr	26.88 Hr	203.21 Hr
	ImageNet-1K					
	AlexNet	VGG	VGG-BN	ResNet-50	ResNext-50	DenseNet-161
Size	233.08 MB	506.83 MB	506.85 MB	97.49 MB	95.48 MB	109.41 MB
Time	190.67 Hr	168.67 Hr	204.27 Hr	238.8 Hr	341.33 Hr	664.53 Hr

Table 6: Evaluated workload model size and training time. Training time is measured when running on 1 V100 GPU. CIFAR-10 is trained with batch size 128 for 320 epochs. ImageNet-1K is trained with batch size 256 for 100 epochs. SWB-300 and SWB-2000 are trained with batch size 128 for 16 epochs.

effective. The additional landscape-dependent noise $\Delta^{(2)}$ in DPSGD, which also depends inversely on the flatness of the loss function (see Eq. 5), is thus critical for the system to find flatter minima in the large batch setting.

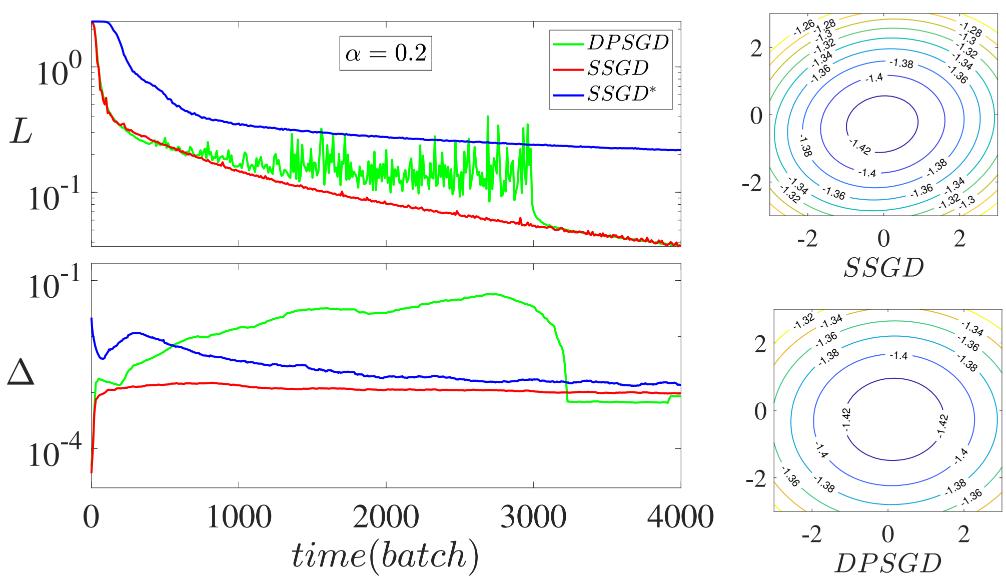

Figure 5: Comparison of different multi-learner algorithms, DPSGD (green), SSGD (red), and SSGD* (blue). For a smaller learning rate $\alpha = 0.2$, both SSGD and DPSGD converge, however, DPSGD finds a flatter minimum with a lower test error than SSGD. The fixed noise SSGD* has the worst performance. See text for detailed description.

D Appendix for Experimental Methodology

D.1 Software and Hardware

We use PyTorch 1.6.0 (Torchvision 0.7.0) as the single learner DL engine. Our communication library is built with CUDA 11.0 compiler, the CUDA-aware OpenMPI 3.1.6, and g++ 8.5.0 compiler. Concurrency control of computation threads and communication threads is implemented via Pthreads. We run our experiments on a cluster of 8-V100 GPU servers. Each server has 2 sockets and 9 cores per socket. Each core is an Intel Xeon E5-2697 2.3GHz processor. Each server is equipped with 1TB main memory and 8 V100 GPUs. Between servers are 100Gbit/s Ethernet connections. GPUs and

CPUs are connected via PCIe Gen3 bus, which has a 16GB/s peak bandwidth in each direction per socket.

D.2 Dataset and Models

We evaluate on three types of DL tasks: CV, ASR and NLP. For CV task, we evaluate on CIFAR-10 dataset [28], which comprises of a total of 60,000 RGB images of size 32 $\times$ 32 pixels partitioned into the training set (50,000 images) and the test set (10,000 images) and ImageNet-1K dataset [5], which comprises of 1.2 million training images (256x256 pixels) and 50,000 (256x256 pixels) testing images. We test CIFAR-10 with 10 representative CNN models [37]. The 10 CNN models are: (1) EfficientNet-B0, with a compound coefficient 0 in the basic EfficientNet architecture [49]. (3) VGG-19, a 19 layer instantiation of VGG architecture [46]. (4) ResNet-18, a 18 layer instantiation of ResNet architecture [14]. (5) DenseNet-121, a 121 layer instantiation of DenseNet architecture [20]. (6) MobileNet, a 28 layer instantiation of MobileNet architecture [19]. (7) MobileNetV2, a 19 layer instantiation of [45] architecture that improves over MobileNet by introducing linear bottlenecks and inverted residual block. (8) ShuffleNet, a 50 layer instantiation of ShuffleNet architecture [62]. (9) GoogleNet, a 22 layer instantiation of Inception architecture [48]. (10) ResNext-29, a 29 layer instantiation of [53] with bottlenecks width 64 and 2 sets of aggregated transformations. The detailed model implementation refers to [37]. Among these models, ShuffleNet, MobileNet, MobileNet-V2, EfficientNet represent the low memory footprint models that are widely used on mobile devices, where federated learnings is often used. The other models are standard CNN models that aim for high accuracy. We test 6 CNN models for ImageNet-1K, AlexNet [29], VGG11 [46], VGG11 with BatchNorm [21] VGG11-BN, ResNet-50 [14], ResNext-50 [53], and DenseNet-161 [20].

For ASR tasks, we evaluate on SWB-300 and SWB-2000 dataset. The input feature (i.e. training sample) is a fusion of FMLLR (40-dim), i-Vector (100-dim), and logmel with its delta and double delta (40-dim $\times$3). SWB-300, whose size is 30GB, contains roughly 300 hour training data of over 4 million samples. SWB-2000, whose size is 216GB, contains roughly 2000 hour training data of over 30 million samples. The size of SWB-300 held-out data is 0.6GB and the size of SWB-2000 held-out data is 1.2GB. The acoustic model is a long short-term memory (LSTM) model with 6 bi-directional layers. Each layer contains 1,024 cells (512 cells in each direction). On top of the LSTM layers, there is a linear projection layer with 256 hidden units, followed by a softmax output layer with 32,000 (i.e. 32,000 classes) units corresponding to context-dependent HMM states. The LSTM is unrolled with 21 frames and trained with non-overlapping feature subsequences of that length. This model contains over 43 million parameters and is about 165MB large.

For NLP task, we evaluate on wikitext-103 dataset [38]. The model architecture is GPT-2 [43], with 16 attention layers, 256 sequence length, 10 attention heads, 410-dimension word embedding , and 2100 hidden dimensions. The vocab size is 28996. Model size is 201.58 MB.

Table 6 summarizes the model size and training time (on 1 V100 GPU) for evaluated tasks. CIFAR-10 tasks train 320 epochs, ImageNet-1K tasks train 100 epochs, and all ASR tasks train 16 epochs.

E Appendix for Results Section

E.1 CIFAR-10 Single Learner Baseline

For CIFAR-10 experiments, we use the hyper-parameter setup proposed in [37]: a baseline 128 sample batch size and learning rate 0.1 for the first 160 epochs, learning rate 0.01 for the next 80 epochs, and learning rate 0.001 for the remaining 80 epochs. Using the same learning rate schedule, we keep increasing the batch size up to 8192. Table 7 in Appendix E records test accuracy under different batch sizes. Model accuracy consistently deteriorates beyond batch size 1024 because the learning rate is too small for the decreased number of parameter updates.

E.2 SSGD and DPSGD Comparison on CIFAR-10

To improve model accuracy beyond batch size 1024, we apply the linear scaling rule (i.e., linearly increase learning rate w.r.t batch size) [14, 12, 60]. We use learning rate 0.1 for batch size 1024, 0.2 for batch size 2048, 0.4 for batch size 4096, and 0.8 for batch size 8192 (except in EfficientNet-B0 batchsize 8192, we use learning rate 0.7). Table 8 compares SSGD and DPSGD performance running

	Batch Size						
	128	256	512	1024	2048	4096	8192
EfficientNet-B0	87.51	89.32	91.28	**91.92**	90.62	88.00	84.85
VGG-19	93.51	**93.78**	93.35	93.12	92.64	91.82	87.76
ResNet-18	**95.44**	95.26	95.08	94.59	94.96	92.98	91.24
DenseNet-121	95.06	95.27	**95.42**	95.11	94.81	93.09	92.34
MobileNet	89.53	90.96	**92.39**	92.24	91.22	89.54	86.59
MobileNetV2	90.52	92.93	94.17	**94.99**	93.71	91.97	89.81
ShuffleNet	90.4	92.27	92.82	**93.15**	91.94	90.59	87.81
GoogleNet	94.99	95.06	94.97	**95.32**	94.05	92.78	91.09
ResNext-29	95.35	**95.66**	95.31	95.42	94.24	93.00	91.06

Table 7: CIFAR-10 accuracy (%) with different batch size. Across runs, learning rate is set as 0.1 for first 160 epochs, 0.01 for the next 80 epochs and 0.001 for the last 80 epochs. Model accuracy consistently deteriorates when batch size is over 1024. Bold text in each row represents the highest accuracy achieved for the corresponding model, e.g., EfficientNet-B0 achieves highest accuracy at 91.92% with batch size 1024.

		Eff-B0	VGG	Res-18	Dense-121	Mobile	MobileV2	Shuffle	Google	ResNext-29
bs=128 lr=0.1	Baseline	87.51	93.51	95.44	95.06	89.53	90.52	90.40	94.99	95.35
bs=1024	SSGD	**91.92**	93.12	94.59	95.11	92.24	**94.99**	93.15	**95.32**	95.42
lr=0.1	DPSGD	91.69	**93.15**	**94.98**	**95.12**	**92.52**	94.36	**93.55**	95.18	**95.72**
bs=2048	SSGD	**91.69**	92.64	**94.96**	95.11	91.72	94.24	**92.91**	94.76	94.19
lr=0.2	DPSGD	91.06	**93.05**	94.86	**95.32**	**92.72**	**94.51**	92.89	**94.80**	**95.30**
bs=4096	SSGD	**91.62**	92.68	94.30	94.72	91.68	**94.25**	**92.67**	94.36	93.21
lr=0.4	DPSGD	91.23	**92.72**	**94.78**	**95.24**	**92.03**	94.12	92.20	**94.99**	**94.32**
bs=8192	SSGD	10	87.11	92.70	92.79	91.10	**93.22**	92.09	93.72	92.38
lr=0.8	DPSGD	**91.13**	**90.52**	**94.34**	**94.79**	**91.80**	93.09	**92.36**	**93.84**	**92.55**

Table 8: DPSGD and SSGD comparison for CIFAR-10, batch size 2048, 4096 and 8192, with learning rate set as 0.2, 0.4 and 0.8 respectively. All experiments are conducted on 16 GPUs (learners), with batch size per GPU 128, 256 and 512 respectively. Bold texts represent the best model accuracy achieved given the specific batch size and learning rate. When batch size is 8192, DPSGD significantly outperforms SSGD. The batch size 128 baseline is presented for reference. bs stands for batch-size, lr stands for learning rate.

with 16 GPUs (learners). SSGD and DPSGD perform comparably up to batch size 4096. When the batch size increases to 8192, DPSGD outperforms SSGD in all but one case. Most noticeably, SSGD diverges in EfficientNet-B0 when the batch-size is 8192. Figure 6 in Appendix E.4 details the model accuracy progression versus epochs in each setting. To better understand the loss landscape in SSGD and DPSGD training, we visualize the landscape with 2D contour projections and 2D Hessian projections in Appendix E.5, using the method from [32]. Results in Appendix E.5 demonstrate that DPSGD can often find flatter optima than SSGD for CIFAR-10 tasks, which is consistent with results for MNIST shown in Appendix C. *Summary* DPSGD outperforms SSGD for 8 out of 9 CIFAR-10 tasks in the large batch setting. Moreover, SSGD diverges on the EfficientNet-B0 task. DPSGD is more effective at avoiding early traps and reaching better solutions than SSGD in the large batch setting.

E.3 CIFAR-10 Hyper-Parameter Tuning

By reducing learning rate in the CIFAR-10 batchsize 8192 case as shown in Table 9, SSGD can escape early traps but still lags behind DPSGD. Bold text in each column indicates the best accuracy achieved for that model across different learning rate and optimization method configurations. DPSGD consistently delivers the most accurate models.

E.4 CIFAR-10 Training Progression

Figure 6 illustrates SSGD and DPSGD comparison for CIFAR-10. SSGD and DPSGD perform comparably up to batch size 4096. When batch size increases up to 8192, DPSGD outperforms SSGD in all but one cases. Noticeably, SSGD diverges in EfficientNet-B0 when batch-size is 8192.

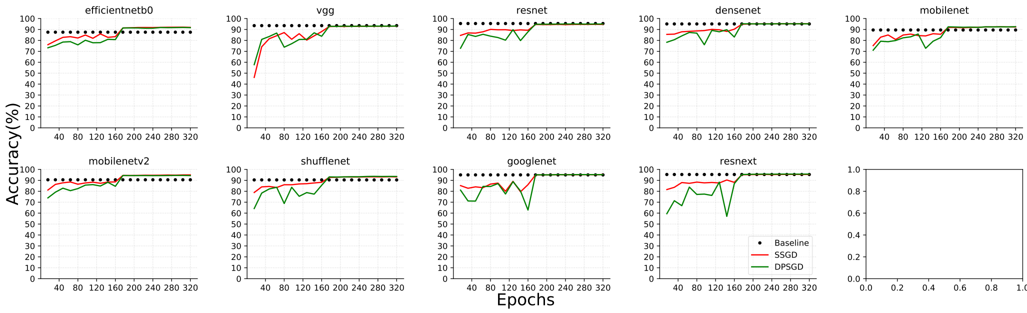

(a) CIFAR-10 convergence, bs=1024, lr=0.1

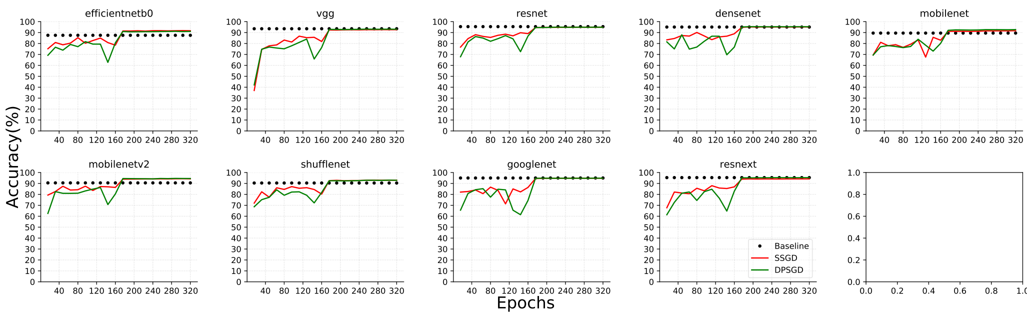

(b) CIFAR-10 convergence, bs=2048, lr=0.2

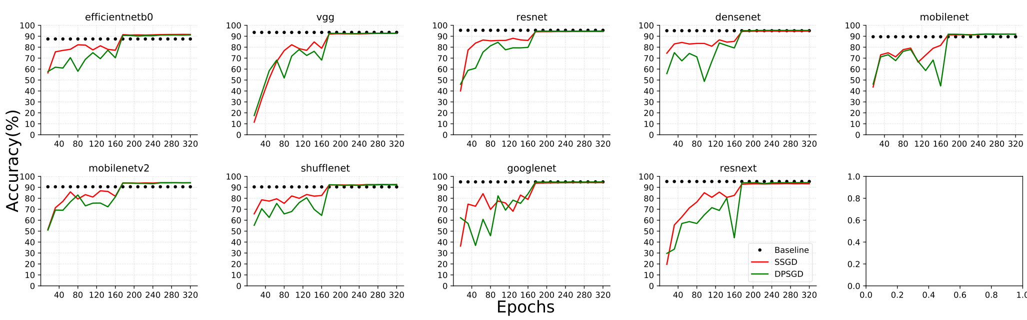

(c) CIFAR-10 convergence, bs=4096, lr=0.4

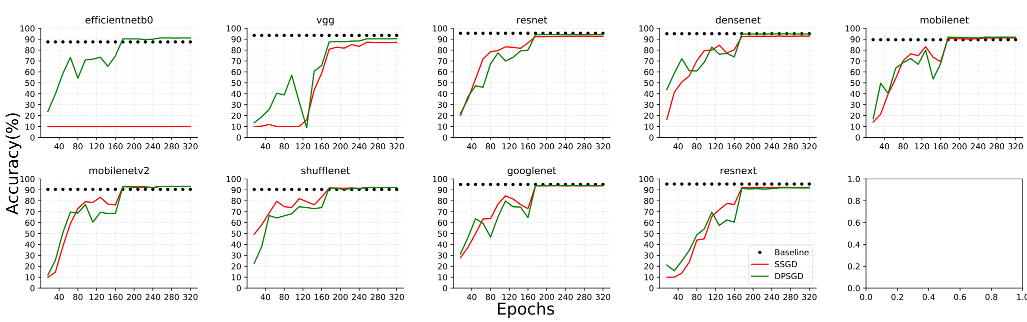

(d) CIFAR-10 convergence, bs=8192, lr=0.8

Figure 6: CIFAR-10 SSGD DPSGD comparison for batch size 2048, 4096 and 8192, with learning rate set as 0.2, 0.4 and 0.8 respectively. All experiments are conducted on 16 GPUs (learners), with batch size per GPU 128,256 and 512 respectively. When batch size is 8192, DPSGD significantly outperforms SSGD. bs stands for batch-size, lr stands for learning rate. The dotted black line represents the bs=128 baseline.

		Eff-B0	VGG	Res-18	Dense-121	Mobile	MobileV2	Shuffle	Google	ResNext-29
lr=0.8	SSGD	10.00	87.11	92.7	92.79	91.10	**93.22**	92.09	93.72	92.38
	DPSGD	**91.13**	90.52	**94.34**	**94.79**	**91.80**	93.09	**92.36**	**93.84**	92.55
lr=0.4	SSGD	88.61	91.06	91.98	93.42	91.13	93.11	91.54	92.85	89.70
	DPSGD	89.80	**91.93**	93.91	94.32	91.38	93.14	91.68	93.49	**92.79**
lr=0.2	SSGD	88.03	90.51	92.13	92.98	88.38	91.68	90.14	92.44	91.31
	DPSGD	87.69	91.59	93.30	94.28	89.18	92.52	90.13	93.41	91.79

Table 9: CIFAR-10 with batch size 8192. By reducing learning rate, SSGD can escape early traps but still lags behind DPSGD. Bold text in each column indicates the best accuracy achieved for that model across different learning rate and optimization method configurations. DPSGD consistently delivers the most accurate models.

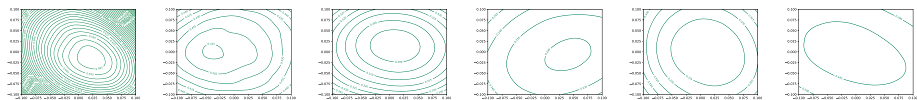

(a) VGG-S (b) VGG-DP (c) ResN-S (d) ResN-DP (e) DenseN-S (f) DenseN-DP

Figure 7: CIFAR-10 2D contour plot. The more widely spaced contours represent a flatter loss landscape and a more generalizable solution. The distance between each contour line is 0.005 across all the plots. We plot against the model trained at the end of 320th epoch. VGG: VGG-19, ResN: ResNet-18, DenseN: DenseNet-121, -S: -SSGD, -DP: -DPSGD

E.5 CIFAR-10 Loss Landscape Visualization

To better understand the loss landscape in SSGD and DPSGD training, we visualize the landscape contour 2D projection and Hessian 2D projection, using the same mechanism as in [32]. For both plots, we randomly select two N-dim vectors (where N is the number of parameters in each model) and multiply with a scaling factor evenly sampled from -0.1 to 0.1 in a $K \times K$ grid to generate K^2 perturbations of the trained model. To produce a contour plot, we calculate the testing data loss of the perturbed model at each point in the $K \times K$ grid. Figure 7 depicts the 2D contour plot for representative models (at the end of the 320th epoch) in a 50×50 grid. DPSGD training leads not only to a lower loss but also much more widely spaced contours, indicating a flatter loss landscape and more generalizable solution. For the Hessian plot, we first calculate the maximum eigen value λ_{max} and minimum eigen value λ_{min} of the model's Hessian matrix at each sample point in a 4x4 grid. We then calculate the ratio r between $|\lambda_{\text{min}}|$ and $|\lambda_{\text{max}}|$. The lower r is, the more likely it is in a convex region and less likely in a saddle region. We then plot the heatmap of this r value in this 4x4 grid. The corresponding models are trained at the 16-th epoch (i.e. the first 5% training phase) and the corresponding Hessian plot Figure 8 indicates DPSGD is much more effective at avoiding early traps (e.g., saddle points) than SSGD.

E.6 ImageNet-1K Training Progression

Figure 9 illustrates SSGD and DPSGD comparison for ImageNet-1K. Noticeably, SSGD diverges in AlexNet, VGG11, VGG11-BN when batch-size is 8192 while DPSGD converges.

E.7 SWB Training Progression

Figure 10 illustrates heldout loss comparison for SWB-300 and SWB-2000. In SWB-300 task, SSGD diverges beyond batch size 2048 and DPSGD converges well til batch size 8192. In SWB-2000 task, SSGD diverges beyond batch size 4096 and DPSGD converges well til at least batch size 8192.

F Appendix: End-to-End Run-time Comparison and Advice for Practitioners

End-to-End Run-time Comparison In all above-mentioned DPSGD and SSGD experiments we used the *same* number of epochs as in the well-tuned single-GPU baseline (i.e., the total computation cost is fixed). When computation cost is fixed, DPSGD inherently runs faster than SSGD because DPSGD requires less messages transmitted and tolerate high-latency network better [33]. Table 11 records training time for each representative task (batch size 128 per GPU, 16 GPUs) on both low and

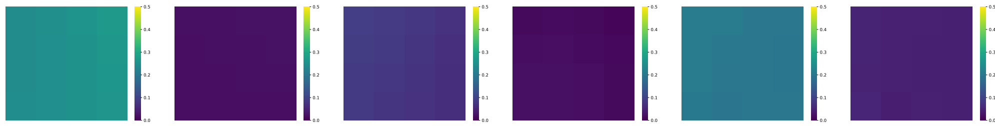

(a) VGG-S (b) VGG-DP (c) ResN-S (d) ResN-DP (e) Dense-S (f) Dense-DP

Figure 8: CIFAR-10 Hessian heatmap on a 4x4 grid. The lower value (i.e. a cooler color) indicates the corresponding point is less likely in a saddle. We plotted against the models at the end of the 16th epoch. DPSGD is much more effective at avoiding early traps (e.g., saddle points) than SSGD. VGG: VGG-19, ResN: ResNet-18, DenseN: DenseNet-121, -S: -SSGD, -DP: -DPSGD

		AlexNet	VGG	VGG-BN	ResNet-50	ResNext-50	DenseNet-161
bs=256	Baseline	56.31/79.05	69.02/88.66	70.65/89.92	76.39/93.05	77.62/93.64	78.43/94.20
lr=1x		lr=0.01		lr=0.1			
bs=2048	SSGD	**54.29/77.43**	**67.67/87.91**	**70.36/89.58**	**76.648/92.99**	**77.486/93.62**	**78.19/94.16**
lr=8x	DPSGD	53.71/76.91	67.28/87.58	69.76/89.31	76.094/92.82	77.236/93.60	77.28/93.64
bs=4096	SSGD	0.10/0.50	0.10/0.50	65.39/86.51	**76.46/93.06**	**77.43/93.65**	**77.98/93.86**
lr=16x	DPSGD	**52.53/76.01**	**66.44/87.20**	**68.86/88.82**	75.784/92.82	77.24/93.54	77.73/93.81
bs=8192	SSGD	0.10/0.50	0.10/0.50	0.10/0.50	**76.096/92.80**	76.564/93.16	**77.34/93.65**
lr=32x	DPSGD	**49.01/73.00**	**65.00/86.11**	**63.55/85.43**	75.618/92.75	**77.162/93.42**	77.22/93.61

Table 10: ImageNet-1K Top-1/Top-5 model accuracy (%) comparison for batch size 2048, 4096 and 8192. All experiments are conducted on 16 GPUs (learners), with batch size per GPU 128, 256 and 512 respectively. Bold texts represent the best model accuracy achieved given the specific batch size and learning rate. The batch size 256 baseline is presented for reference. bs stands for batch-size, lr stands for learning rate. Baseline lr is set to 0.01 for AlexNet and VGG11, 0.1 for the other models. In the large batch setting, we use learning rate warmup and linear scaling as prescribed in [12]. For rough loss landscape like AlexNet and VGG, SSGD diverges when batch size is large whereas DPSGD converges.

high latency networks. Other tasks and batch-size setups show the same trend: DPSGD runs faster than SSGD. Further note that for Eff-B0 (target accuracy 90%) and SWB-2000 (target heldout loss 1.48), DPSGD reaches target model quality with twice the batch size as used in SSGD, all learning rates considered (Table 9 , Table 4). Thus DPSGD can effectively use 2X more GPUs. DPSGD achieves target accuracy for Eff-B0 in 0.067 hours and for SWB-2000 in 10.08 hours (64 GPUs). In contrast, SSGD achieves target accuracy for Eff-B0 in 0.19 hours and for SWB-2000 in 23.15 hours (32 GPUs).

In addition, DPSGD is immune to stragglers, while approaches that require global synchronization suffer slowdowns. Figure 11 demonstrates when there is a learner running 5x slower than other learners, DPSGD converges much faster than LAMB[55], a state-of-the art SSGD based large-batch training solution, on the SWB300 task. This experiment demonstrates that even SSGD-variant algorithms (e.g., LAMB) can be designed to work for specific training tasks, DPSGD can simultaneously tackle the convergence problem and straggler-avoidance problem for the generic large batch training tasks.

Summary DPSGD consistently runs faster than SSGD to reach target accuracy in the large batch setting.

		Eff-b0	Res-18	Dense-121	Mobile	Google	ResNext-29	SWB-2000
	Single-GPU	2.92	1.37	5.48	1.02	5.31	4.55	203.21
Latency ($1\mu s$)	SSGD	0.34	0.35	0.68	0.17	0.58	0.56	38.00
	DPSGD	0.26	0.32	0.58	0.12	0.49	0.41	29.71
Latency ($1ms$)	SSGD	0.46	0.82	0.96	0.30	0.84	0.94	96.31
	DPSGD	0.27	0.32	0.58	0.13	0.50	0.42	29.85

Table 11: Time (hours) to complete training with batch size 128 per GPU and 16 GPUs in total (CIFAR-10 and SWB-2000).

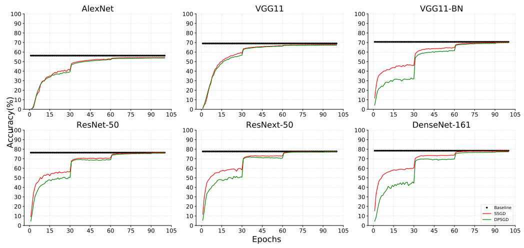

(a) ImageNet-1K Top-1, bs=2048, lr=8x

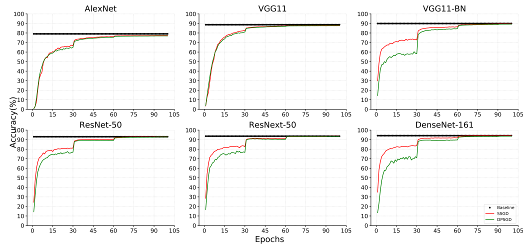

(b) ImageNet-1K Top-5, bs=2048, lr=8x

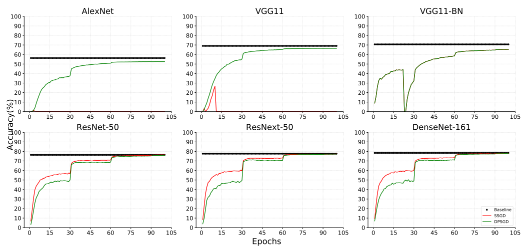

(c) ImageNet-1K Top-1, bs=4096, lr=16x

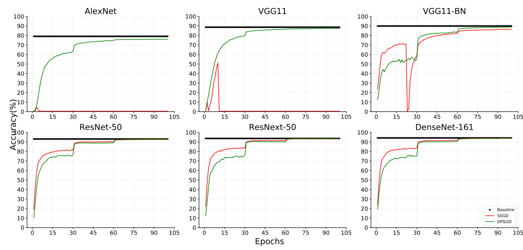

(d) ImageNet-1K Top-5, bs=4096, lr=16x

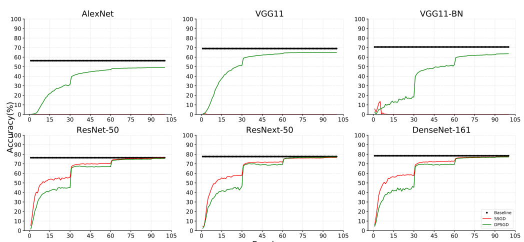

(e) ImageNet-1K Top-1, bs=8192, lr=32x

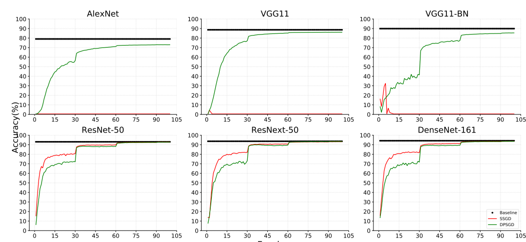

(f) ImageNet-1K Top-5, bs=8192, lr=32x

Figure 9: ImageNet-1K SSGD DPSGD comparison for batch size 2048, 4096 and 8192, with learning rate set as 0.2, 0.4 and 0.8 respectively. All experiments are conducted on 16 GPUs (learners), with batch size per GPU 128,256 and 512 respectively. When batch size is 8192, DPSGD significantly outperforms SSGD. bs stands for batch-size, lr stands for learning rate. The dotted black line represents the bs=256 baseline.

Advice for Practitioners In SSGD, when total batch size is fixed, the convergence behavior is the same regardless of the number of learners. In DPSGD, when the number of learners increases, the convergence could be harmed due to too much discrepancy between learners. In another word, we would like a system that has enough system noise so that it can help avoid early training traps but not too much noise so that model convergence is unaffected. In practice, we found that 16-learner setup usually yields the best convergence results in the DPSGD setting, which is consistent with research literature [33, 34]. To make use of a larger number of computing devices in DPSGD, we recommend a hierarchical system design [58] where we group nearby learners (e.g., on the same server) as one big super-learner and apply DPSGD algorithm only across super-learners. For example, on a 128 GPU cluster, we could group 8 learners as one big super-learner and we apply DPSGD among 16 super-learners. In addition, we also recommend in each iteration, each (super)-learner selects a random neighbor to communicate to further improve convergence. Please refer to [59] for the detailed analysis of how randomized communication improves DPSGD convergence.

G Related Work

To increase parallelism in DDL, one must increase batch size, which often leads to a deteriorating model accuracy [61, 30]. Meticulous task-specific learning rate tuning for large batch training exists in CV training [12, 54], NLP training [55] and ASR training [57]. Among them, layer-wise adaptive

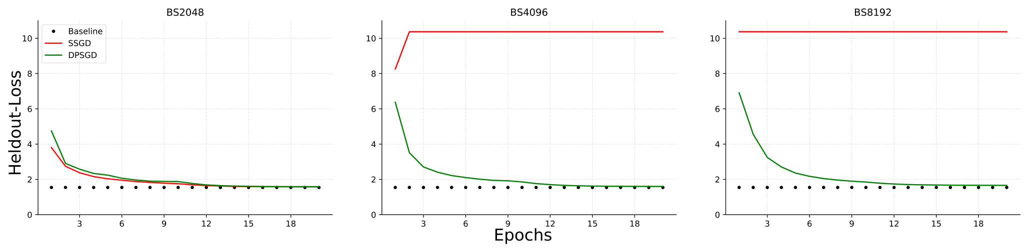

(a) SWB300

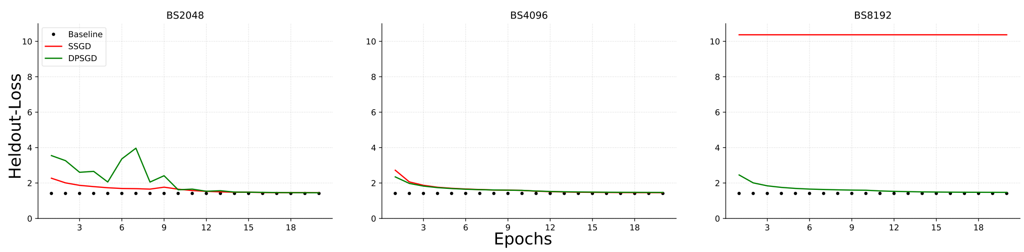

(b) SWB2000

Figure 10: Heldout loss w.r.t epochs for SWB-300 and SWB-2000. Dotted black lines indicate the batch size 256 heldout loss baseline.

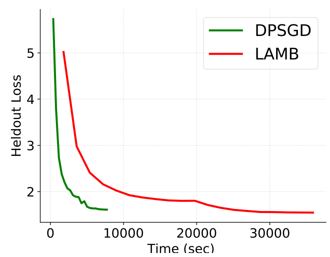

Figure 11: LAMB (a state-of-the-art SSGD based solution) and DPSGD comparison when there is a straggler that runs 5x slower than other learners in the system. SWB-300 task, batch size 4096, x-axis is running time and y-xais is the held-out loss.

learning rate tuning schemes [54, 55] rely on the Adam optimizer [25], which may diverge on some simple convex functions [44]. In particular, [54, 55] requires every learner to see other learner's gradients to calculate the large minibatch gradient, [9] optimizes both original loss function and the sharpness of the minimization, [35] calculates extra-gradient information and [51] leverages the covariance matrix of gradients noise. Furthermore, all above-mentioned approaches require global synchronization and suffer from the straggler problem: one slow learner can slow down the entire training process.The noise in the stochastic gradient plays an important role in terms of generalization performance in deep learning. Keskar et al. [24] show that large batch training procedures usually find sharp minima with poor generalization performance. This phenomenon is analyzed from different perspectives, including PAC-Bayesian learning theory [40, 41, 7], stochastic differential equation [22], Bayesian inference [47] and optimization theory [26]. There are several efforts trying to design algorithms to find flat minima that generalize better than SGD [2, 23].